

AD-A039 598

TEXAS INSTRUMENTS INC DALLAS EQUIPMENT GROUP
JOSEPHSON JUNCTION TECHNOLOGY PROGRAM. PHASE I.(U)
APR 77 F D COLEGROVE, S A BUCKNER

F/G 9/1

UNCLASSIFIED

N00173-76-C-0388

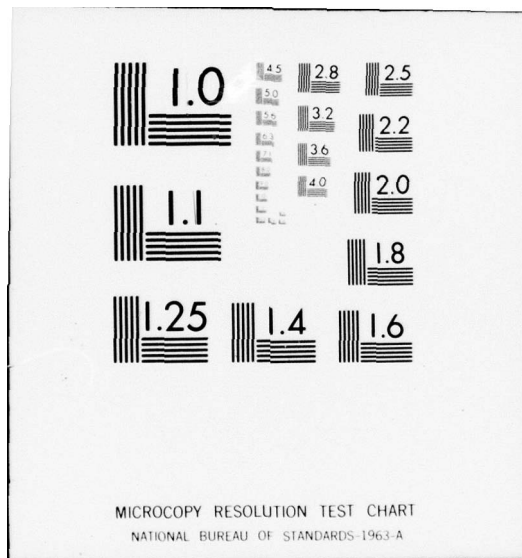
NL

1 OF 1
ADA039 598



END

DATE
FILMED
6-77



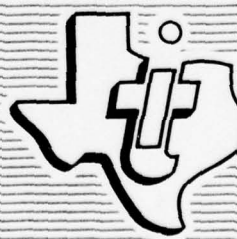
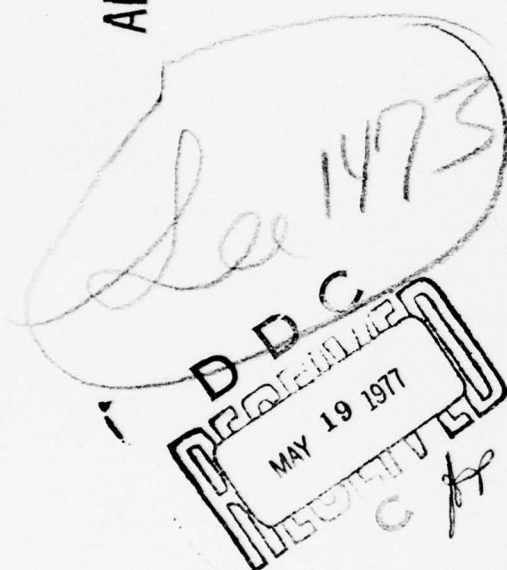
AD No. 1

DDC FILE COPY



ADA 039598

12



TEXAS INSTRUMENTS
INCORPORATED

(12)

JOSEPHSON JUNCTION TECHNOLOGY
PROGRAM
PHASE I

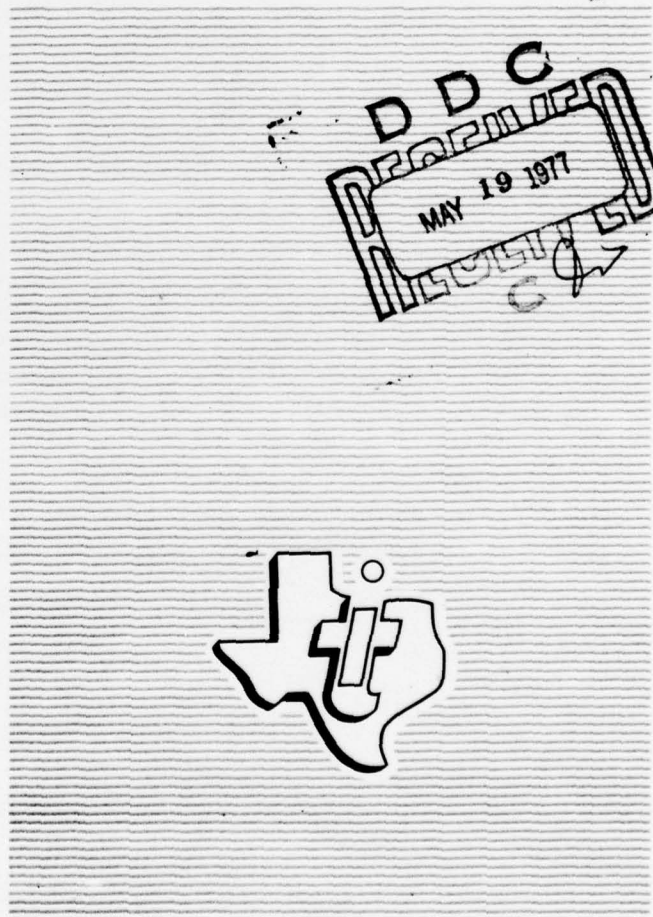
Prepared for:

Naval Research Laboratory
Cryogenics and Superconducting
Branch
Code 6435
Washington, D.C. 20375

Prepared by:

Texas Instruments Incorporated
Equipment Group
P.O. Box 6015, MS 266
Dallas, Texas 75222

Final Report for
Contract No. N00173-76-C-0388
21 April 1977



TEXAS INSTRUMENTS
INCORPORATED



TABLE OF CONTENTS

Section	Title	Page
I	INTRODUCTION	1-1
II	APPLICATIONS SURVEY	2-1
	A. Josephson Device Capabilities Summary	2-4
	1. SQUID's	2-4
	2. RF Detectors	2-8
	3. Computer Elements	2-14
	B. DC to 10 Hz	2-16
	1. Sensitivity	2-16
	2. Processing	2-18
	C. 10 Hz to 1 kHz	2-20
	D. 1 kHz to 1 GHz	2-23
	1. Receiving Systems	2-23
	2. Real Time Correlation Processing for Spread Spectrum Applications	2-24
	E. 1 GHz - 100 GHz	2-30
	1. Overview	2-30
	2. Radar System Considerations	2-33
	3. Communication Receiver	2-37
	4. Electronic Warfare Applications	2-40
	5. 94 GHz Radiometer	2-43
	6. Processing for Radar Imagers	2-45
	F. Above 100 GHz	2-45
III	CONCLUSIONS AND RECOMMENDATIONS	3-1
	APPENDIX A (Two page, classified appendix with separate limited distribution)	



SECTION I

INTRODUCTION

A search has been made of Naval surveillance and communication systems to identify any for which the unique properties of Josephson effect devices might improve system performance. The search was broadened slightly to include non-Josephson sensors employing superconductors, the most important one being the super-Schottky diode. Some system and component categories were eliminated from detailed consideration by general arguments related to their requirements and the known characteristics of superconducting devices. However practical considerations related to refrigeration, size, weight, power and cost were not used as a basis to reject potential applications since significantly improved system performance could justify a compromise in these factors and also lead to development activities that could greatly change what is a relatively new technology.

Comparisons have been made between present and projected performance of existing systems and the projected performance of systems employing superconducting phenomena. Known potential applications (magnetic anomaly detection for anti-submarine warfare and ELF communications) have been included as well as those systems where the comparison was unfavorable.

The principle new areas of application are at microwave frequencies, the most promising one employing video detection in millimeter wavelength systems. For some applications, an imaging system at these frequencies could improve the resolution of existing radar images and still have good penetrability through atmospheric particulates.

The general conclusions are that Josephson effect devices will most likely be used at very low frequencies (<10 kHz), very high frequencies (>10 GHz) and for fast digital processing.



SECTION II

APPLICATIONS SURVEY

Identification of potential applications for Josephson effect devices requires assumptions of projected capabilities of these devices. An initial literature search was made to compare the performance level achieved by various Josephson effect devices to the theoretical limit. Three categories of device applications were considered: SQUID's, detectors and digital processing components. Included in the data on coherent and incoherent Josephson detectors are super-Schottky diodes and some cooled conventional detectors. This capabilities summary will be given first.

Early in the survey, it became evident that certain classes of potential applications could be eliminated without detailed analysis because present systems are limited in performance by the environment in which they operate rather than by components of the system itself. In many systems where some improved performance is still possible, it can be achieved by somewhat more sophisticated conventional components that are still far simpler to use than Josephson devices. This situation applies mainly to detection methods at middle frequencies and will be treated in the appropriate subsections.

In addition, certain classes of components rely on characteristics not generally associated with Josephson devices. For instance, most signal sources are designed for relatively high power output, such as klystrons, magnetrons, traveling wave tubes, backward wave oscillators, cross field amplifiers, power vacuum tubes and even solid state devices and lasers. Josephson devices, which may be used as local oscillators in mixer applications, are very low power components and the amplifier which would be required to obtain useful transmitting power could itself be used as the source. Josephson sources as local oscillators should be considered in conjunction with Josephson or super-Schottky heterodyne detection systems.



The only way in which transmitting and receiving antennas or antenna structures might be influenced by Josephson effect devices would be the potential size reduction made possible by lower noise in receivers. At frequencies below a few hundred hertz the magnetic field is often measured instead of the electric field. In military applications this is done either by measuring the current induced in a loop or coil of wire (with or without a ferromagnetic core) or by the direct effect of the field on electrons in a material, such as in the resonance magnetometers or Hall probes. At somewhat higher frequencies the electric field is measured by currents induced in a tuned circuit or a long conductor which is much shorter than the wavelength measured.

Antennas throughout the rest of the electromagnetic spectrum generally consist of a conductor in some configuration with dimensions of the order of the wavelength to be measured such as

- Vertical towers
- Half wave dipoles
- Loops
- Rhombics
- Discones
- Helical antennas
- Parasitic arrays
- Slots
- Log Periodics
- Antenna arrays
- Wave guides

Many times these are used in conjunction with reflecting surfaces for focusing on small antennas. In a few cases superconductors may replace ordinary conductors in the antenna loops, coils, etc., as, for instance, in some magnetometers and gradiometers. Josephson devices may be used as the sensing element for measuring the small currents induced in these



antennas but no techniques have been identified to use Josephson effect devices to enhance the performance of the antenna itself. Their use as detectors and amplifiers is treated in appropriate subsections.

One way in which Josephson devices might directly influence antenna design would be an application in which it is very important to make the antenna much smaller than normal. For a radar system the antenna size will be determined by required beamwidth, weight limits, physical location, and range-power requirements. The availability of a lower noise receiver system would provide more trade-off flexibility. However, the only systems where low noise Josephson devices coupled with superconducting antenna elements would uniquely allow a small antenna design are "supergain" arrays. These are discussed in the 1 KHz to 1 GHz subsection.

In a communications system some minimum sized antenna is required to receive the signal and background noise at a level adequate for overcoming internal receiver noise. A receiver system with a 20°K noise temperature could operate with an effective antenna area 50 times smaller than one with a 1000°K noise temperature. Loran and Omega are examples of systems that require fairly large antennas to assure background limited operation. However, no systems have been identified where reduction in antenna size is of sufficient importance that cooled detectors or other more conventional techniques have been employed in an effort to reduce antenna size.

The remainder of this section will be devoted to characterization of some Josephson devices and consideration of specific potential applications including some that have been considered and rejected.



A. Josephson Device Capabilities Summary

1. SQUID's

Superconducting quantum interference devices (SQUID's) for measuring magnetic fields have been made in various forms both in research laboratories and commercially. At the present time there are two companies in the United States making SQUID's: S.H.E. Corporation, 4174 Sorrento Valley Blvd., San Diego, California, and Superconducting Technology, Inc. (ScT), 1400 Stierlin Road, Mountain View, California. The SQUID's made by these two companies are RF SQUID's operating at approximately 30 MHz. The most extensive work on DC SQUID's has been done by Professor John Clarke's group at the University of California at Berkeley. Table 1 summarizes the properties of the SQUID's of these three groups.

The parameters tabulated in Table 1 can be understood from the schematic diagram of a SQUID and superconducting transformer coupled to the SQUID to form a magnetometer or gradiometer shown in Figure 1. The flux transfer ratio for this circuit is

$$\phi_s/\phi_p = N_p M / (L_p + L_i) ,$$

or in terms of the SQUID coupling factor k

$$\phi_s/\phi_p = N_p k \sqrt{L_i L_s} / (L_p + L_i) .$$

Here N_p is the number of turns in each pickup coil. Optimizing the above equation with respect to L_i gives the result that $L_i = L_p$ for maximum flux transfer. The optimum flux transfer ratio is then

$$(\phi_s/\phi_p)_{\max} = N_p k \sqrt{L_s/L_i} / 2 = N_p M / 2L_i .$$

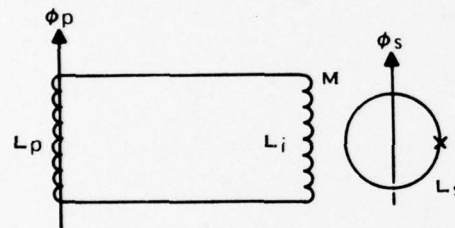


Table 1: Properties of Representative SQUID SYSTEMS

	ϕ_{rms}	M	L_i	$N_p \phi_{\text{rms}}$	E_{ni}
ScT thin film RF SQUID	$1.3 \times 10^{-4} \phi_0 / \sqrt{\text{Hz}}$	6.9nH	280nH	$1 \times 10^{-2} \phi_0 / \sqrt{\text{Hz}}$	$2 \times 10^{-28} \text{ J/Hz}$
ScT toroidal point contact RF SQUID	3×10^{-5}	4	600	9×10^{-3}	7×10^{-29}
SHE model 330 RF SQUID	2×10^{-4}	20	2000	4×10^{-2}	4×10^{-28}
SHE model 330 X RF SQUID	7×10^{-5}	20	2000	1×10^{-2}	5×10^{-29}
Clarke cylindrical thin film DC SQUID*	3.5×10^{-5}	11.5	356	2×10^{-3}	7×10^{-30}
Clarke planar thin film DC SQUID*	8×10^{-5}	1	1.7	$3 \times 10^{-4}**$	2×10^{-29}

* J. Clarke, W. M. Goubau, M. B. Ketchen, J. Low Temp. Phys. 25, 99 (1976).

** Since ϕ_{rms} is calculated under the assumption that the pickup coils are perfectly matched to the SQUID input coil ($L_p = L_i$), this number is not meaningful for the Clarke planar thin film DC SQUID. Because of the extremely low value of input inductance, L_i , the ratio L_i / L_p cannot in practice be made much greater than $\sim .005$. This value would give $N_p \phi_{\text{rms}} = 3 \times 10^{-2} \phi_0 / \sqrt{\text{Hz}}$.



L_p = TOTAL INDUCTANCE OF PICKUP COILS
 L_i = INDUCTANCE OF SQUID INPUT COIL
 L_s = INDUCTANCE OF SQUID
 $M = K\sqrt{L_i L_s}$ = MUTUAL INDUCTANCE
BETWEEN INPUT COIL AND SQUID

Figure 1. Schematic Diagram of Superconducting Transformer and SQUID



The minimum rms magnetic field fluctuation at the pickup coils that can be detected by a SQUID with an rms flux noise of ϕ_s rms can be calculated from the above equation:

$$N_p \phi_p \text{ rms} = N_p A_p B_{\text{rms}} = 2L_i \phi_s \text{ rms} / M.$$

The quantities tabulated in Table 1 are ϕ_s rms, M, L_i , $N_p \phi_p \text{ rms}$, and the SQUID noise energy referred to the input coil, $E_{ni} = L_i (\phi_s \text{ rms} / M)^2 / 2$. As shown in Table 1 values of the flux noise at the pickup coils of 0.2 to $1 \times 10^{-2} \phi_0 / \sqrt{\text{Hz}}$ are representative of what has been achieved to date. For 5 cm diameter one-turn pickup coils this corresponds to sensitivities of 0.2 to 1×10^{-14} T at one pickup coil.

A simple derivation of the intrinsic limit of sensitivity of a SQUID set by Johnson noise in the SQUID is the following.¹ A DC SQUID, biased so as to be resistive at all times, is approximated by a loop of inductance L and resistance $R' = 2R$ where R is the normal state resistance of each junction. The mean-square noise current generated in the loop is then

$$\overline{i^2} = \overline{v^2} / Z^2 = 4kT R' B / (R'^2 + \omega^2 L^2).$$

The mean-square flux noise is

$$\overline{\phi^2} = L^2 \overline{i^2} = 4kT R' L^2 B / (R'^2 + \omega^2 L^2).$$

In the low-frequency limit $\omega \ll R/L$ and

$$\overline{\phi^2} = 4kT L^2 B / R'.$$

For $L = 10^{-9}$ H, $R' = 2\Omega$, and $B = 1$ Hz,

$$\phi_{\text{rms}} = 5 \times 10^{-6} \phi_0.$$



This is a factor of 7 better than the best value reported by Clarke for his DC SQUID's.

An RF SQUID is effectively resistive only during the time $\tau \sim L/R$ required for the flux state to change.¹ Only during this period is thermal noise current important. This reduces the effective averaging time by a factor of the order of $\omega\tau = \omega L/R$ so that for an RF SQUID

$$\overline{\phi^2} = 4kTLB/\omega .$$

The theoretical sensitivity increases with increasing frequency and approaches the value for the DC SQUID as ω approaches R/L . For $\omega = 2 \times 10^8$ sec⁻¹, $B = 1$ Hz, and $L = 1$ nH (typical of cylindrical SQUIDS),

$$\phi_{rms} = 2 \times 10^{-5} \phi_0 .$$

The SHE and ScT toroidal SQUID's have inductances on the order of 0.1 nH. For this case

$$\phi_{rms} = 5 \times 10^{-6} \phi_0 .$$

2. RF Detectors

Josephson devices have been studied rather extensively as broadband detectors and as heterodyne mixers. Kanter and Vernon² have shown that the broadband response can be divided into three characteristic-frequency regions depending on whether the internal self-generated Josephson frequency, $\omega_0 = 2eV/\hbar$, is larger than, equal to, or smaller than the signal frequency, ω . For $\omega_0 \ll \omega$ they found that the response is proportional to (1) the slope of the DC I-V characteristic, (2) the inverse square of the signal frequency, (3) the inverse of the bias current expressed as a multiple of the critical current, and (4) the voltage amplitude of the inherent Josephson oscillations. For $\omega_0 \gg \omega$ "classical" detection proportional to the curvature, d^2V/dI^2 , of the I-V characteristic was found.



For $\omega_0 \sim \omega$ a type of resonance detection occurs which depends to a considerable degree on fluctuations of the average voltage across the device. Most of the data available on Josephson video detectors has been limited to the first regime, $\omega_0 \ll \omega$, and this is the data on video detectors that has been plotted in Figure 2. The theoretical curve for Josephson video detectors shown in Figure 2 was taken from Reference 2 with optimum parameter values assumed for a Nb point contact device.

The most common mixing mode that has been studied in Josephson devices involves a very small signal current at a frequency very close to an external local oscillator frequency. The local oscillator and signal in this case are equivalent to a slowly amplitude-modulated wave of average amplitude I_{lo} and modulation depth I_{sig}/I_{lo} . When a sufficiently large-amplitude local oscillator signal is applied to a Josephson device, the zero-voltage current of the device is suppressed and current steps appear on the I-V characteristic at voltages $V_n = n\hbar\omega/2e$. The effect, then, of an amplitude-modulated local oscillator signal is to cause the I-V characteristic to move up and down at the difference frequency (IF) between local oscillator and signal. The IF voltage can be found from pairs of I-V characteristics for slightly different RF current amplitudes. The IF response is proportional to the dynamic resistance dV/dI of the I-V characteristic at the bias point and to the variation of the zero-voltage current with RF current amplitude. This behavior is in contrast to the conventional mixer in which the response is proportional to d^2I/dV^2 .

Data for Josephson mixers operating in this mode as well as room-temperature and cooled conventional Schottky-barrier diodes and super-Schottky diodes are included in Figure 2. The super-Schottky diode is an ordinary Schottky diode in which the normal metal has been replaced with a superconducting metal. The super-Schottky is therefore a low-temperature device and is influenced by the presence of the superconductor

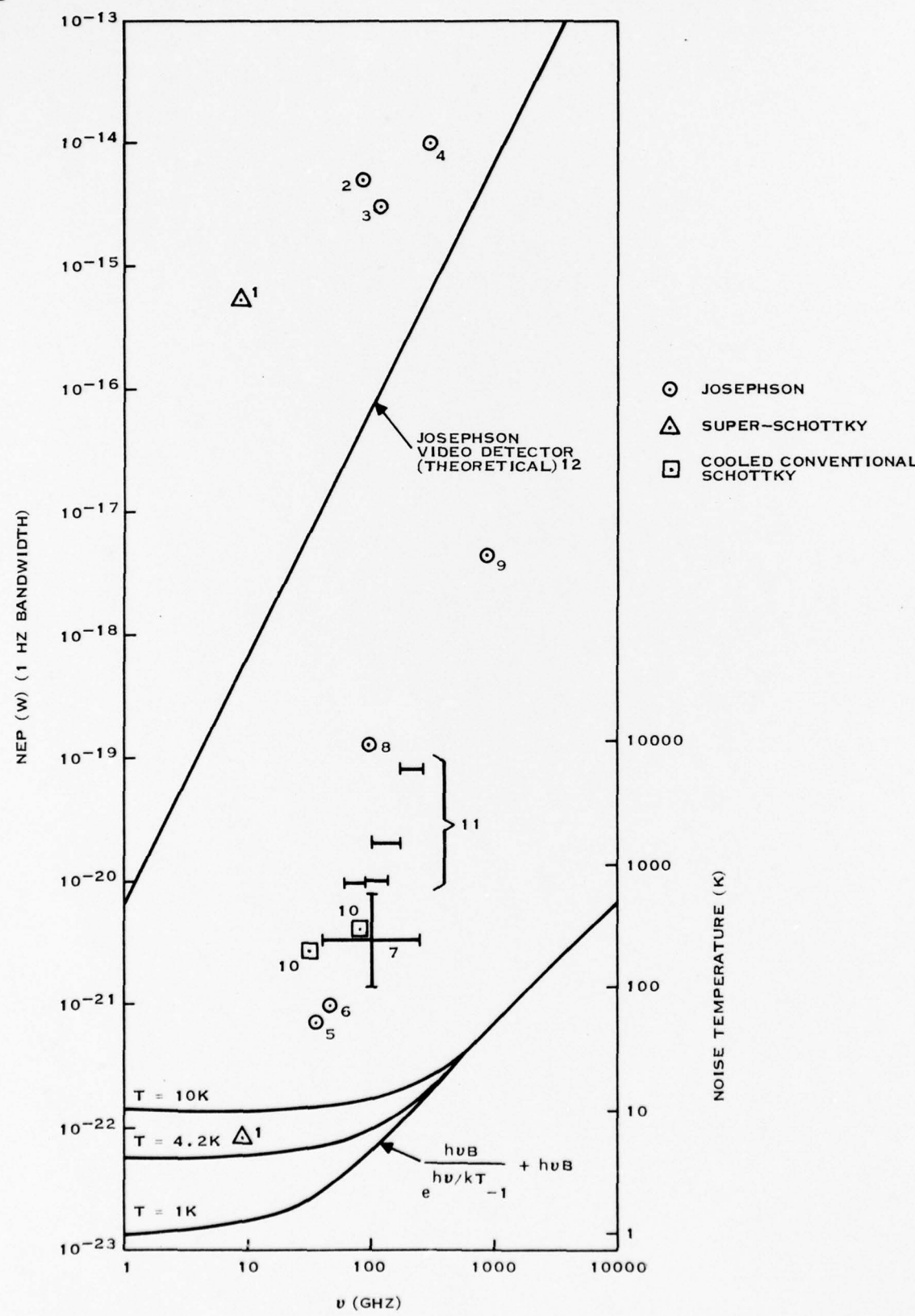


Figure 2. Comparison of Theoretical and Experimental Capabilities



References for Data of Figure 2

1. M. McColl, M.F. Millea, A.H. Silver, M.F. Bottjer, R.J. Pedersen, F.L. Vernon, IEEE Trans. Magnetics MAG-13, 221 (1977). p-GaAs, $T = 1.06\text{K}$, 9 GHz, $\text{NEP} = 5.4 \times 10^{-16} \text{ W/}\sqrt{\text{Hz}}$
p-GaAs, Pb super-Schottky mixer
 $T = 1.06\text{K}$, 9 GHz, $T_{\text{mixer}} = 6 \text{ K}$ ($\text{NEP} = 8.3 \times 10^{-23} \text{ W/Hz}$), $L_C = 7 \text{ dB}$
2. H. Kanter, F.L. Vernon, J. Appl. Phys. 43, 3174 (1972).
Nb Josephson point contact
 $T = 4.2 \text{ K}$, 90 GHz, $\text{NEP} = 5 \times 10^{-15} \text{ W/}\sqrt{\text{Hz}}$
3. H. Tolner, C.D. Andriesse, H.H.A. Schaeffer, Infrared Phys. (G.B.) 16, 213 (1976).
Josephson point contact
120 GHz, $\text{NEP} = 3 \times 10^{-15} \text{ W/}\sqrt{\text{Hz}}$
4. B.T. Ulrich, Proc. 12th Int. Conf. Low Temp. Phys. (Kyoto, Japan, 1970), p. 867.
Nb Josephson point contact
300 GHz, $\text{NEP} = 10^{-14} \text{ W/}\sqrt{\text{Hz}}$
5. Y. Taur, J.H. Claassen, P.L. Richards, IEEE Trans. Microwave Theory and Techniques MTT-22, 1005 (1974).
Nb Josephson point contact
 $T = 8\text{K}$, 36 GHz, $T_{\text{mixer}} = 260\text{K}$ ($\text{NEP} = 3.6 \times 10^{-21} \text{ W/Hz}$), $G_C = 7.6 \text{ dB}$
 $= 210\text{K}$ ($\text{NEP} = 2.9 \times 10^{-21} \text{ W/Hz}$), $L_C = 4.2 \text{ dB}$
 $T = 4.2\text{K}$, 36 GHz, $T_{\text{mixer}} = 140\text{K}$ ($\text{NEP} = 1.9 \times 10^{-21} \text{ W/Hz}$), $L_C = 2.2 \text{ dB}$
 $= 120\text{K}$ ($\text{NEP} = 1.7 \times 10^{-21} \text{ W/Hz}$), $L_C = 2.0 \text{ dB}$
V Josephson point contact
 $T = 1.4 \text{ K}$, 36 GHz, $T_{\text{mixer}} = 55\text{K}$ ($\text{NEP} = 7.6 \times 10^{-22} \text{ W/Hz}$), $L_C = 1.4 \text{ dB}$
 $= 54\text{K}$ ($\text{NEP} = 7.5 \times 10^{-22} \text{ W/Hz}$), $G_C = 2.5 \text{ dB}$
6. J. Edrich, IEEE Trans. Microwave Theory and Techniques MTT-24, 706 (1976).
Nb Josephson point contact
 $T = 4.2\text{K}$, 47 GHz, $T_{\text{mixer}} = 71\text{K}$ ($\text{NEP} = 9.8 \times 10^{-22} \text{ W/Hz}$), $L_C = 12.3 \text{ dB}$
7. R.S. Avakjan, A.N. Vystavkin, V.N. Gubankov, V.V. Migulin, V.D. Shtykov, IEEE Trans. Magnetics MAG-11, 838 (1975).
Nb point contact mixer using intrinsic Josephson oscillation as local oscillator
 $T = 4.2\text{K}$
40-260 GHz, $T_{\text{mixer}} = 100\text{-}600\text{K}$, $L_C = 8\text{-}12 \text{ dB}$

8. H. Kanter, Rev. Phys. Appl. 9, 255 (1974).

Nb Josephson point contact

$$T = 4.2K, 95 \text{ GHz}, T_{\text{mixer}} = 49100K \quad (\text{NEP} = 6.78 \times 10^{-19} \text{ W/Hz}), L_C = 21 \text{ dB}$$

$$= 33900 \quad (\text{NEP} = 4.68 \times 10^{-19} \text{ W/Hz}), L_C = 24 \text{ dB}$$

$$= 32900 \quad (\text{NEP} = 4.55 \times 10^{-19} \text{ W/Hz}), L_C = 23 \text{ dB}$$

$$= 15500 \quad (\text{NEP} = 2.14 \times 10^{-19} \text{ W/Hz}), L_C = 19 \text{ dB}$$

$$= 11700 \quad (\text{NEP} = 1.62 \times 10^{-19} \text{ W/Hz}), L_C = 21 \text{ dB}$$

9. T.G. Blaney, Rev. Phys. Appl. 9, 279 (1974).

Nb point contact mixer

$$T = 4.2K, 891 \text{ GHz}, T_{\text{mixer}} = 3.27 \times 10^5 K \quad (\text{NEP} = 4.5 \times 10^{-18} \text{ W/Hz}), L_C = 29 \text{ dB}$$

10. S. Weinreb, A.R. Kerr, IEEE J. Solid-State Circuits SC-8, 58 (1973).
cooled (15K) Schottky barrier mixer

frequency	T_{mixer}	T_{receiver}	L_C
33 GHz	200K	260K	5.8 dB
85	280	350	7.2

11. A.A. Penzias, Rev. Phys. Appl. 9, 7 (1974).

room temperature Schottky barrier mixers

frequency band	T_{receiver}
60-90 GHz	700 K
90-140	750
110-170	1500
170-260	6000

12. Theoretical Response of Josephson Video Detector (Reference 2).

$$\text{NEP} (\omega_0 \ll \omega) = \frac{n(8e)^{1/2} I_c^{3/2}}{R I_c^2} \left(\frac{h}{2e} \right)^2 v^2 \quad (\text{W}/\sqrt{\text{Hz}}) \quad \omega_0 = \frac{2eV}{\hbar}$$

$$\text{Let } n = 1, I \approx I_c, R I_c = \frac{\pi \Delta}{2e}, \Delta_{\text{Nb}} = 1.5 \text{ meV}, I_c \approx 10 \mu\text{A}.$$

$$\text{NEP} = \frac{(8e)^{1/2} I_c^{1/2}}{\frac{\pi \Delta}{2e}} \left(\frac{h}{2e} \right)^2 v^2$$



only in the voltage range corresponding to the superconducting energy gap. Its operation is otherwise similar to that of conventional Schottky-barrier diode mixers. (Its mixing properties depend on the nonlinearity of the I-V characteristic.)

The sensitivity limit of a coherent receiver can be written as the sum of two terms, one due to thermal (Johnson) noise and the other due to quantum noise:

$$NEP = h\nu B / (e^{h\nu/kT} - 1) + h\nu B .$$

This expression has been plotted in Figure 2 for $T = 1, 4.2$, and $10K$.

Several different modes of parametric amplification in Josephson devices have been studied both experimentally and theoretically. A Josephson parametric upconverting amplifier which is self-pumped by internal Josephson oscillations produced by a dc voltage bias has been built and tested.³ A Nb point contact SQUID was simultaneously coupled to a 115 MHz tank circuit and a 9 GHz cavity. Josephson oscillations at 9 GHz produced parametric upconversion of power in the 115 MHz circuit to sidebands at 9 ± 0.115 GHz with a measured power gain of 25 (14 dB). The amplifier noise temperature referred to the input at 115 MHz was less than 15K.

In another system gain of 12 dB at 10 GHz was observed in a parametric amplifier whose nonlinear element was a series of unbiased microbridges (tin).⁴ The operating temperature of the system was 2.61K. The bandwidth was measured to be 1 GHz and the noise temperature to be less than 20 K.

Silver⁵ has described the possibility of using a Josephson junction as a parametric upconversion amplifier (from 1 GHz to 61 GHz) in conjunction with a super-Schottky diode to frequency downconvert the amplified signal back to 1 GHz. This system was proposed as the



first stage of IF amplification in a 100 GHz receiver system using a super-Schottky mixer to convert the 100 GHz signal to 1 GHz. He has calculated that such an IF amplifier should have a noise temperature near 1K and a gain of 9 dB.

Use of Josephson devices as oscillators would seem feasible only as local oscillators in conjunction with other superconducting devices used as mixers. Silver⁵ describes the use of Josephson junctions phase-locked to a harmonic of an RF standard signal as the local oscillator in his 100 GHz receiver system. The junctions would be voltage-biased at approximately 200 μ V to generate a 100 GHz signal and would have to generate 10^{-9} W. He calculates that frequency stability of a part in 10^6 should be possible.

3. Computer Elements

The potential of Josephson tunnel junctions as computer elements has been well established. Requirements which a computer element must meet are that it be a fast switch, dissipate little power, occupy a small volume, and be able to be manufactured cheaply and with high yield in large arrays with very high packing density. Some switching times for Josephson tunnel junctions which have been reported in the literature are tabulated below:

Junction Area	Rise Time of Voltage Transition	
$3.1 \times 10^4 \mu\text{m}^2$	<800 psec	(Ref 6)
1.2×10^4	60	(Ref 7)
1.7×10^2	<24 theoretical value: 6 psec	(Ref 8)

It would seem that junction switching times on the order of a few picoseconds should eventually be obtainable.



For devices that have been reported so far, the junction switching time is not the limiting time for a Josephson logic element. Two Josephson tunnel junctions can be used to make a memory cell that has nondestructive readout and that can be incorporated into a random access memory. Representative write times and energy dissipation that have been reported are the following:

Junction Area	Write Time	Energy Dissipation
$9.4 \times 10^3 \mu\text{m}^2$	600 psec	$2 \times 10^{-15} \text{ J}$ (Ref 9)
2.0×10^1	80	10^{-16} (Ref 10)

Such memory cells can be combined to perform logic functions and arithmetic operations. Representative times for such devices that have been reported are:

AND, OR, INVERT, CARRY logic functions: logic delay of 200 psec;
power delay product $\sim 5 \times 10^{-15} \text{ J}$ (Ref 11)

One-bit adder: Logic delay of 500 psec (Ref 12)

Four-bit multiplier: multiplication time of 27 nsec (Ref 13)



B. DC to 10 Hz

Josephson junctions are ideally suited for use as the "weak links" in superconducting quantum interference devices (SQUIDs). These devices are presently being considered by the Navy as sensors in potentially improved systems for airborne detection of magnetic anomalies. In both cases the source of the signal is the distortion of the earth's magnetic field by a ferromagnetic object otherwise hidden from view. In the present detection method the earth's magnetic field strength is monitored by an observer in an aircraft. When field strength changes characteristic of the sensor passing over an anomaly are observed, the aircraft flies a pattern designed to determine precise location.

Fast detection and localization is becoming increasingly important in operations employing MAD sensors. Any increase in range would be helpful. However, of possibly greater value would be information of the exact location and approximate orientation of the anomaly obtained on the first contact. Such information can only be determined by measuring the magnetic field gradients instead of just the scalar magnitude. For equal range this generally requires greater sensor sensitivity and/or large separation of the sensors.

1. Sensitivity

The magnetic field strength, B_m , of a dipole of moment M at a distance r_m is proportional to M/r_m^3 . The magnetic field gradient is therefore proportional to M/r_m^4 . Published estimates show that when the dipole field strength of a typical target is 0.1 nT, the gradient is about 3×10^{-4} nT/M.^{1,2} Conventional magnetometers with sensitivities of about 10^{-2} nT could be used as gradiometers but would only have adequate sensitivity if separated by about 30 metres. In a compact gradiometer with sense loop separation of 20 cm, the required field sensitivity at each loop would be about 7×10^{-5} nT.



Five cm diameter pickup loops with SQUID sensors have been shown to have sensitivities of 2×10^{-6} nT. This sensitivity is about 35 times better than that required to give a detection range equal to that of conventional magnetometers. This factor of 35 improvement in sensitivity would correspond to an increase in detection range of $(35)^{1/4} = 2.4$ in the absence of environmental gradient noise. The theoretical limit was shown to be another factor 7 better than has been achieved experimentally. However external magnetic gradient noise will most likely limit detection ranges. The calculated range based on instrument noise gives the maximum range due to intrinsic SQUID noise.

Two geometrical conditions must be met to use this sensitivity in a gradiometer. The inductance of the two pickup coils must be the same and their axes must be parallel (or the coils must be coplanar). The criteria to determine whether these conditions are adequately met is that the largest change in field which occurs during normal operation should not induce signals in the gradiometer circuit larger than the gradiometer noise level. The field change in a particular direction may be as much as 10^5 nT during maneuvers, but is probably less than 10^3 nT during straight runs. Therefore the sensitivity to uniform field changes should be less than 7.5×10^{-5} nT/ 10^3 nT $\sim 1 \times 10^{-7}$ of the sensitivity of each loop. Such precision can be obtained by deposition of superconducting film patterns on quartz substrates. Pattern edges can be positioned to within 2.5 μm . However the average dimensions of the two loops will probably be better.



How much better is important since the stable, fabricated balance of four-centimeter-diameter loops can be assured to within less than one part in 5×10^5 using this value but may actually be much closer to the part in 10^7 required.

Small scale irregularities in the substrate surface will average and therefore not affect the axis direction. However, departure from flatness over distances comparable to the dimensions of the gradiometer coils will cause misalignment of the two coil axes in each of the perpendicular directions. For a flatness of $\pm \delta$, over the dimensions of a coil the angular misalignment of the axes could be as much as δ/r . Gradiometer loops misaligned by this amount appear to be a magnetometer of area $\pi r^2 \sin(\delta/r)$ for a change in magnetic field perpendicular to the gradiometer axis. Surface flatness can be readily controlled to 5×10^{-5} cm and with some care down to 10^{-5} cm. The ratio of sensor loop area to effective magnetometer area from misalignment for a 4 cm loop can be made 4×10^5 or greater. To achieve a factor of 10^7 in gradient sensitivity relative to field sensitivity may require compensation.

2. Processing

Wynn¹⁴ has shown that observations of the complete gradient field at a single point in space can locate the position and orientation of a dipole source. According to the method of Wynn, the azimuth angle of the position vector is the solution of a six degree polynomial. The coefficients of this polynomial are an elaborate algebraic combination of five independent dipole field gradients. The polar angle and components for the magnetic moment are then obtained in a straightforward manner from other formulas involving the field gradients. A uniqueness proof of Wynn's solution, based upon the theory of sixth-degree polynomials^{15,16} could be difficult.

Gradient measurements can be used both for target location and discrimination by indicating whether the source is a dipole. At Texas Instruments a proprietary processing technique has been defined which is somewhat simpler and provides a unique solution.



Some magnetic signal processing schemes¹⁷ have been directed toward extraction of tactical parameters from a time history of scalar magnetometer measurements taken from a moving platform. The gradient method, on the other hand, combines outputs from several sensors at each point in time. This makes real time tracking a possibility. Overton¹⁸ makes a case based upon signal to noise considerations for a single moving gradiometer. However, extracting information from the temporal waveform from a single gradiometer would be more difficult than extracting information from magnetometer signals because the gradient signal requires four basis functions to represent it, rather than three as in the magnetometer case. Otherwise, the processing methods would be much the same. The signals from five gradient sensors on one moving platform can be combined to form a temporal signature that is represented by a single basis function. This greatly simplifies the signal processing and parameter extraction is possible with only a small portion of the track. Problems of platform stability must also be considered in both system design and processing.¹⁹

While work on gradiometer signal processing techniques is only in its earliest stages, it appears reasonable to assume that very useful information can be extracted from gradiometer signals. Gradient information with a reasonably sized sensor can only be obtained with the high sensitivity demonstrated by SQUID sensors which use the Josephson device as the critical element.



C. 10 Hz to 1 kHz

The frequency range from 10 to 200 Hz is of great interest in communicating with submerged submarines. Existing antennas are extremely long (hundreds of meters) and are limited in performance by various factors. The stated magnetic field sensitivity for H-field antennas for ELF communication systems is about 10^{-14} T/Hz^{1/2} referred to air, which is well within the operational sensitivity of present generation SQUIDS coupled to flux transformers with several-centimeter-diameter primaries. Thus, a configuration of SQUIDS that is relatively insensitive to orientation with respect to the earth's field might be used as a substitute for the present ELF antennas.

In April 1963, the Navy conducted a communication demonstration between a shore based ELF (30-300 Hz) radio transmitter located in N.C. and a nuclear submarine operating at a range of 3200 Km with its receiving antenna near keel depth. Termed the "Intensive Test", this event established the fact that a deployed submarine could receive messages from the continental United States without its receiving antenna being on or near the surface of the ocean. After this demonstration, early investigations showed that certain kinds of ELF waves propagate through the earth-ionosphere cavity and penetrate to considerable depths inside sea water.²⁰

The feasibility of such a system (Project Sanguine) has been emphasized in numerous papers²¹ with the conclusion that there is no fundamental technical reason why such a system is not feasible.

In order to achieve omnidirectionality present E-field receiving antennas consist of towed electrode pairs which greatly restrict the maneuverability of the submarine. The alternatives are to deploy a wire perpendicular to the trailing antenna, which is impractical, or to trail an H-field antenna.



In the particular case of the proposed Sanguine ELF communications system, a submarine ELF H-field sensor must have a sensitivity equal to or greater than -200 dB relative to $1 \text{ V/m/Hz}^{1/2}$ in a bandwidth 100 Hz wide, centered at a frequency of 80 Hz.²² The bandwidth requirement will permit wideband noise processing to reduce the impact of the highly non-Gaussian noise in the ELF band on the communications signal. Furthermore, present solenoid sensors cannot satisfy the noise requirements for adequate performance in likely operating areas with the planned ELF transmitting capacity and the required message rate. Therefore, trying to supplement the E-field trailing wire antenna with an H-field antenna of the ferromagnetic core solenoid type in order to achieve omnidirectionality runs into the problem of having a sensitivity that is about 30 dB worse than the required performance.

In view of the above, perhaps a new approach seems warranted. The required sensitivity of $10^{-14} \text{ T/(Hz)}^{1/2}$ should be achievable with a SQUID system coupled to a superconducting flux transformer. The flux transformer consists of two coils made of a continuous simply connected wire or ribbon of superconducting material. One coil is coupled inductively to the SQUID cylinder and the other coil is exposed to the external flux. If the external field is changed, a current will flow in the superconducting flux transformer to keep the enclosed flux constant, thus producing a corresponding change in the field at the SQUID. Such devices have been built²² and signals of the order of $10^{-14} \text{ T/(Hz)}^{1/2}$ can readily be detected.

One of the most serious problems in utilizing the $10^{-14} \text{ T/(Hz)}^{1/2}$ sensitivity of a SQUID device is the spurious signal generated by the device moving in the earth's magnetic field of $0.5 \times 10^{-4} \text{ T}$. Because the earth's field is uniform on the physical scale of a typical SQUID, a set of three orthogonal sensors can be used to sum the vector components continuously and thus permit the large earth's field component to be removed as a dc component.



The problem areas in this approach are:

1. Providing enough dynamic range in the parts of the system ahead of the vector summing stage to prevent the SQUID electronics from being saturated, and
2. Achieving orthogonality among the sensors.

The total dynamic range requirement is about 194 dB. However, using techniques that have been developed for magnetic airborne detection, physical rotation of the sensor can be constrained to less than 10^{-3} rad, thus lowering the dynamic range requirement to about 134 dB. Present-day SQUID electronics have a dynamic range of 140 dB. The 134 dB dynamic range and 100 Hz bandwidth can be achieved by using 24-bit digital electronics and a 9.6 KHz sampling rate.

Since a reasonable goal for platform stability is 10^{-3} rad (already achieved in operational airborne MAD systems) the sensors must have effective orthogonality to 10^{-4} rad. Therefore, a subsidiary alignment procedure or an alignment servo mechanism should be incorporated. A conceptually simple method of incorporating such a compensation scheme has been proposed by Wolf, Davis and Nisenoff.²²

Other SQUID configurations should be studied, for example a gradiometer mode of detection, since the ELF signal might have appreciable gradient signature. It may be possible to separate the earth's magnetic field noise from the signal of interest very effectively in a gradiometer type detector. In this case there would be no stringent orthogonality requirement on the detectors, but rather a stringent alignment requirement in the gradiometer coils. All of these are unexplored, and require further investigation.



D. 1 kHz to 1 GHz

1. Receiving Systems

In this frequency range conventional, room temperature components are sufficiently well developed that front end receivers can be designed to contribute less than 2 dB to system noise. In an application where this small improvement would be important, it is likely that cooled conventional components could be used more easily.

A compact antenna using active devices may be an attractive alternative to conventional antennas in some instances. Studies have been made of the feasibility of using a Josephson magnetometer to collect the H field of an RF wave (in contrast to the conventional method of collecting the E field). Welker and Bedard have shown²³ that it is possible to have a sensitivity of 3.3 fT with a dynamic range of 50 dB and instantaneous bandwidth from DC to 30 MHz for an antenna of this type. The sensitivity of this antenna is much greater than the random noise at some frequencies. The wide bandwidth and relatively small antenna size of an H field antenna might find application in some covert surveillance application, but no specific system has been identified.

Another potential use of superconducting antenna elements, possibly in conjunction with Josephson devices, is in compact array configurations ("super-directive arrays").²⁴ These systems require elements with low internal noise, well matched responses and a size sufficiently small that mutual interaction can be neglected. Superconductive elements may be able to meet these conditions.²³ Supergain arrays are usually dismissed as impractical because of the large counter flowing currents in adjacent elements and the losses associated with these currents. The successful development of superconducting arrays might lead to applications in certain covert operations or in some aircraft where size limitations prevent use of a conventional antenna.



2. Real Time Correlation Processing for Spread Spectrum Applications

Systems which employ direct sequence spread spectrum modulation (such as the joint services programs, GPS and JTIDS) have a common problem which must be solved before they will function properly. This problem is called code synchronization. The conventional correlator performs sequential comparisons of the internally generated code with the coded incoming signal to determine the correct phase match. If there are N chips in the code cell, it could take up to N/v seconds to establish the correct phase, where v is the chip rate, typically about 5-10 MHz.

A real time correlator would employ a parallel comparison of many phases simultaneously, thereby decreasing acquisition time. This technique requires that the sums and the integration occur in each 100 ns chip interval. Present TTL logic with about 10 ns switching times is not fast enough to perform the minimum number of operations required by the parallel processing. Josephson effect cryotrons have demonstrated switching times less than 200 ps¹¹ with one reported value of 24 ps⁸. With these speeds, logic circuits could be developed to implement the parallel, real time correlator. This would decrease acquisition time and/or allow the use of longer codes. Both performance improvements are desirable and for an available processing speed a trade-off would have to be made between the two for each application.

In a system employing direct sequence spread spectrum modulation the transmitter combines a relatively slow data bit stream with a much faster PN code bit stream for purposes of jamming rejection and improved range resolution. A similar code generator in the receiver must be aligned in phase with the apparent signal code phase as it arrives at the receiver. The only thing which is available to indicate when the local code generator comes into alignment with the signal is the magnitude of the signal envelope which is shown in Figure 3.

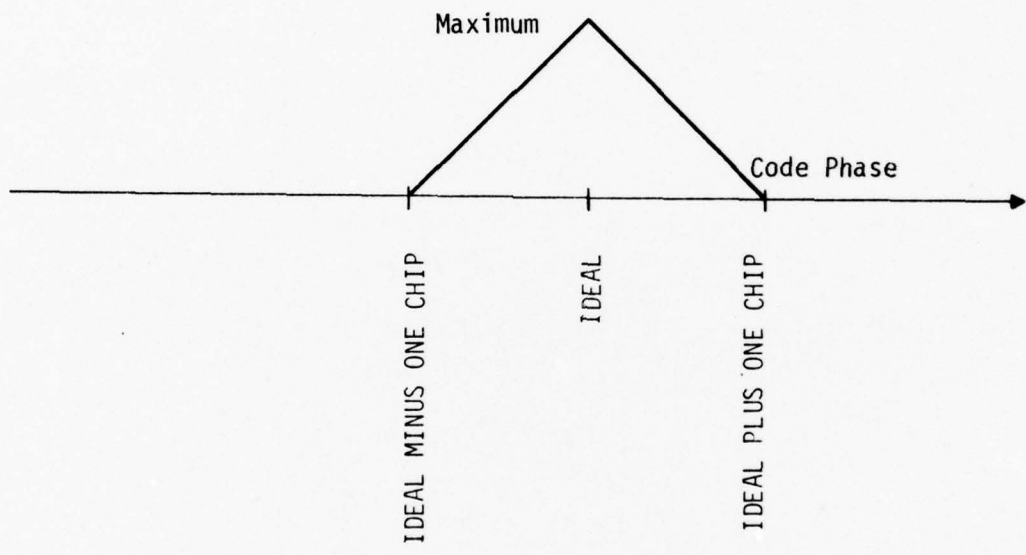


Figure 3. Signal Envelope Magnitude of a Decoded Data Stream as a Function of Encode and Decode Generator Phase Match



This figure shows that the signal envelope falls off linearly with code phase error out to one code chip where it has vanished entirely. Typically, the chip rate can be 5 MHz to 10 MHz so that a chip interval is 100 nanoseconds to 200 nanoseconds. This means that a code generator phase error in excess of 200 nanoseconds results in the complete absence of any signal component to be used for any purpose whatsoever. This necessitates a rather lengthy acquisition procedure during which time all possible code phase uncertainty must be searched for the presence of the signal. This problem is quite analogous to the classic radar pulse detection problem where hypothesis testing is used to achieve required message detection and message dismissal probabilities.

The conventional approach is shown in Figure 4. The search procedure consists of the following tasks:

- 1) The first code phase cell is selected by positioning the code generator to the appropriate initial conditions and then normal clocking is begun,
- 2) The code phase is thus held constant while integration of I & Q components is performed,
- 3) The correlation envelope $E = \sqrt{I^2 + Q^2}$ is obtained and compared to a threshold,
- 4) Failure to exceed threshold indicates lack of true signal phase, thus the code phase is incremented and the integration procedure repeated at the new value of code phase,
- 5) Successful threshold crossing indicates possible presence of signal. A sequence of further integrations is performed in making a final decision as to signal presence/absence.

NOTE: The procedure just described has the property that only one code phase cell is being searched at a time. Thus a relatively large uncertainty in code phase will result in a lengthy sequential search procedure before the true signal code phase is found. This is highly undesirable in its operational implications.

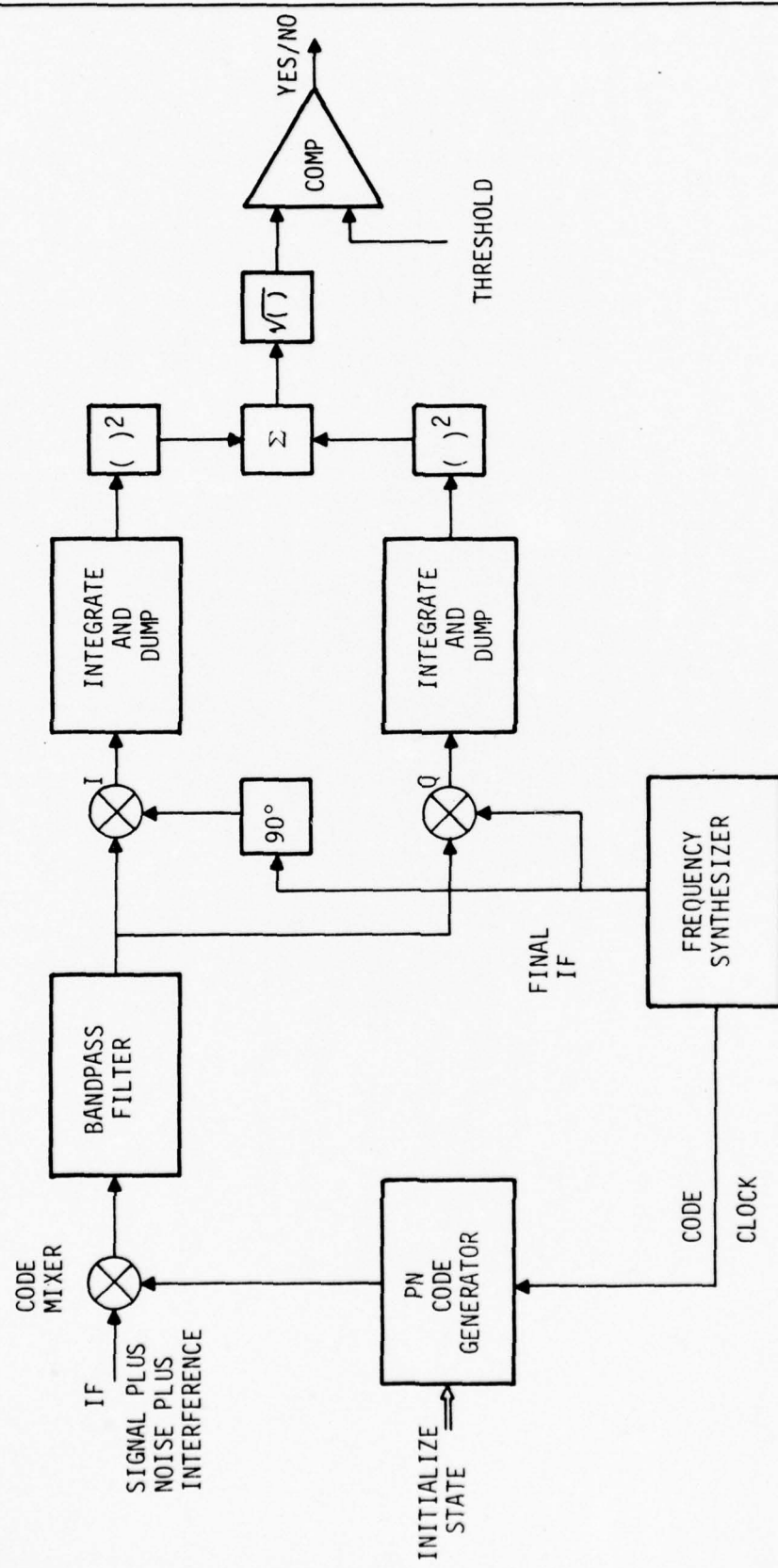


Figure 4. Conventional Code Phase Search System Configuration



The speed potential of Josephson components suggests the system configuration shown in Figure 5. Josephson analog-to-digital converters are used to sample I & Q waveforms directly at IF at a rate greater than or equal to the PN code chip rate, say 5 to 10 MHz. These binary words are processed as shown in such a way as to search N code phase cells simultaneously. Each code bit is used to increment or decrement the accumulator contents by the word from the ADC. The I and Q words are combined at each code phase position according to the equation

$$E_i = \sqrt{I_i^2 + Q_i^2}$$

in order to obtain the correlation envelope value for that particular value of code phase. All the E_i values are compared to a threshold in a hypothesis test similar to that discussed in the conventional approach.

The Josephson technology approach of Figure 5 is superior to the conventional approach of Figure 4 because it tests $N + 1$ code phase cells for presence of the signal in essentially the same time that the conventional scheme requires to test one code phase cell. Thus, acquisition speed is larger by a factor of $N + 1$ which is extremely important for some applications.

If the blocks which make up the digital portions of Figure 5 were distinct interconnections of hardware items, then this approach would almost certainly be impractical because of its required size and complexity. However, the speed potential of Josephson technology logic should permit all of this to be accomplished with one analog-to-digital converter (ADC) and one processor with memory. The accumulators and the shift register are simply memory locations. The ADC must sample both I and Q filter outputs at a rate at least as great as the PN code chipping rate (say 5 MHz to 10 MHz). Then many additions and subtractions of these two samples must be performed according to the scheme of Figure 5.

If these speeds can be realized in Josephson technology logic, then a real contribution can be made to direct sequence, spread spectrum communication receivers for programs such as GPS and JTIDS.

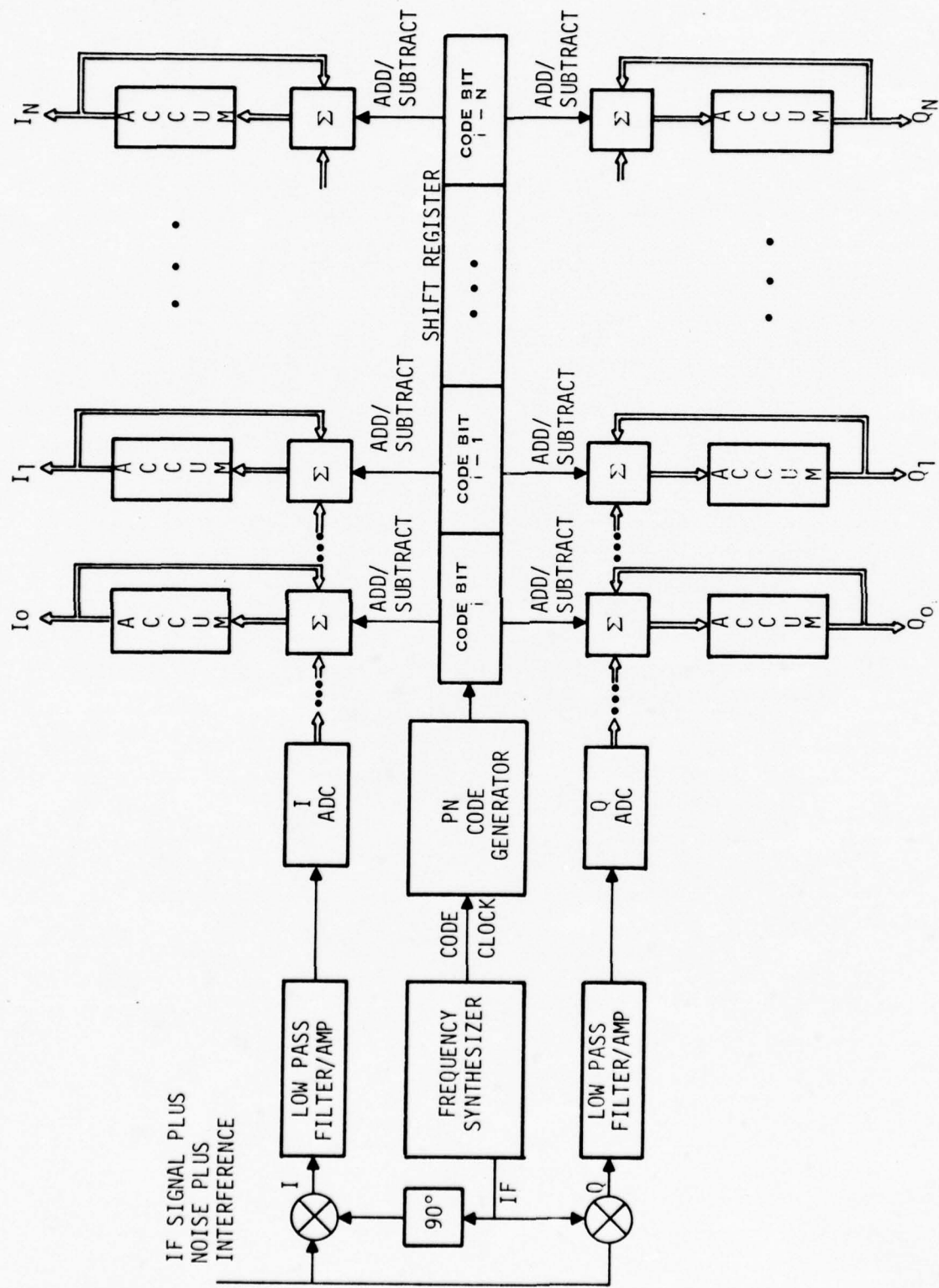


Figure 5. Parallel Code Phase Search System Configuration



E. 1GHz - 100 GHz

1. Overview

The objective of this part of the Phase I study effort has been to examine potential applications of Josephson effect devices and super-Schottky diodes (Schottky diodes using superconducting metal) to Navy communications and surveillance systems, and to identify systems operating between 1 GHz to 100 GHz which are candidates for increased effectiveness through the use of this technology.

The nonlinear properties of Josephson devices are exploitable in several ways to perform electronic functions that can be applied to communications and surveillance systems in the frequency range of interest. Four functions were identified as appropriate for consideration. These functions are:

1) video detectors which operate as incoherent detectors (power detectors), 2) heterodyne mixers which multiply two RF signals to produce a difference frequency (coherent detectors), 3) local oscillators derived from the internally generated Josephson oscillation that occurs when voltage-bias is applied, and 4) parametric amplifiers utilizing the parametric inductance characteristic to achieve gain. Super-Schottky diodes can be used as video detectors and mixers. A summary of the advantages and limitations associated with the application of these devices to the circuit functions described above is presented in Table 2.

Table 2
Summary of Applicable Device Characteristics

<u>Function</u>	<u>Advantage</u>	<u>Limitation</u>
Video Detector	Low Noise Equivalent Power Fast Response Time	Low Saturation Level
Heterodyne Mixer	Low Mixer Temperature	High Conversion Loss Low Saturation Level
Oscillator	Wide Tuning Band	Poor Spectral Characteristics Low Power Level
Parametric Amplifier	Low Noise	Minimum Dynamic Range



Video detectors have been fabricated that use both Josephson and non-Josephson (super-Schottky) technology. Noise equivalent power (NEP) measurements on super-Schottky detectors have demonstrated values as low as 5.4×10^{-16} watts/ $\sqrt{\text{Hz}}$ at 9 GHz²⁵. A conventional uncooled Schottky-diode will achieve typical best case values of 6.3×10^{-13} watts/ $\sqrt{\text{Hz}}$ at this frequency. An improvement of 30.7 dB could be realized by using the super-Schottky detector. The effective RF input bandwidth for these detectors is determined by the structures which couple the RF energy to the junction. Bandwidths of 40 percent should be achievable with junction impedances in the 25 to 75 ohms range. Response times of the order of picoseconds for Josephson devices and nanoseconds for Schottky devices are realized. This is several orders of magnitude faster than those for bolometers. A major limitation to the application of both Josephson and super-Schottky video detectors is associated with the low saturation level. If it is assumed that deviation from square-law response for a video detector occurs at signal levels 10-20dB below optimum local oscillator power levels for the device when it is used as a mixer, then Josephson video detectors deviate from square-law response above -80 to -70 dBm²⁶ and super-Schottky video detectors above -67 to -57 dBm²⁵. Conventional detectors show deviation from square-law response at signal levels above -10 dBm. The maximum energy level that can be handled without permanent device degradation is an important parameter when considering system applications. This information was not available in the literature for these devices.

Heterodyne mixers have been fabricated with Josephson and super-Schottky devices used as the active element. These mixers have displayed low noise temperature performance. Both conversion gain and loss have been observed. Y. Taur et.al.²⁶ reported a mixer noise temperature of 54 K with an associated conversion gain of 2.5 dB at 36 GHz in Josephson point contacts. M. McColl et.al.²⁵ reported a mixer noise temperature of 6 K with an associated conversion loss of 7 dB at a frequency of 9 GHz in super-Schottky diodes. In general, the results reported in the open literature indicate that conversion gain in Josephson devices is achieved at the expense of noise temperature and vice versa. Both parameters influence the overall noise performance of a heterodyne mixer system. Conventional "quiet" mixers exhibit noise temperatures of 200 K with an associated conversion loss of 4 dB. The lower mixer noise



temperature provided by the superconducting devices compares favorably with conventional mixers; however, as is the case with video detectors, the mixers display saturation characteristics at extremely low levels (-70 dBm for Josephson mixers²⁶). A receiver system using such a mixer would suffer a severe penalty in instantaneous dynamic range. In comparing superconducting mixer noise performance with conventional low noise RF preamplifier approaches to achieve minimum receiver noise, the mixer conversion loss plays a limiting role. In this type of comparison, the mixer is pressed to demonstrate any performance improvement. The maximum power handling capability of the Josephson mixer is not known; however, it is suspected to be several orders of magnitude less than conventional mixer diodes (+24 dBm).

Preliminary consideration was given to using the internally generated Josephson oscillation as a voltage tunable local oscillator. The extreme tuning sensitivity (483.6 MHz per microvolt) and low bias voltage conditions (20 μ V for 10 GHz oscillation) result in spectrum broadening to an unusable degree. In addition, the low output power (\approx -50 dBm) from a single device could only be used as a local oscillator source for a Josephson mixer. For these reasons, Josephson oscillator applications were not considered practical.

Parametric amplifiers can be designed that use the nonlinear inductance associated with the Josephson effect. A doubly degenerate parametric amplifier was built to operate at 9 GHz²⁷. The paramp achieved a gain of 10 dB with an associated noise temperature of 20 K. The amplifier saturated at an output power level of -84 dBm. Cooled conventional parametric amplifiers can achieve 40 K noise temperatures at 9 GHz with one dB gain compression at -20 dBm. The modest improvement in noise temperature is offset by the low saturation level, and it is felt that use of the parametric inductance effect to achieve amplification will not be competitive with conventional techniques in the frequency range of interest.

An applications matrix was generated in the early stages of the study. The matrix was used to guide the investigation of specific communications and surveillance systems that could achieve greater effectiveness through the application of Josephson technology. The matrix was arranged to display the



various system categories that could be considered as entries in the left-hand column, and the subsystem/device function that could be performed by Josephson effect devices as entries in the top row. The matrix is shown in Table 3.

The "0" entries designate applications that looked promising after a preliminary study and justified additional investigation. the "X" entries denote potential applications of superconducting device technology that were initially considered and then eliminated as lacking any clear advantage in performance over current techniques.

The following sections of this report on the 1 GHz through 100 GHz task will present the results of the studies conducted on several system categories. The next section considers the general class of radar systems and concludes that little if any performance advantage could be realized. The following section is concerned with electronic warfare systems. Improvement in anti-radiation missile (ARM) seeker detection range can be realized; however, the practical application of Josephson technology to this system has significant physical limitations. The next section deals with applications to communication systems. A satellite communication receiver is analyzed and the results presented. The final section considers a 94 GHz receiver system and concludes that applications of this type represent the most favorable possibility.

2. Radar System Considerations

Improved radar receiver RF assemblies could contribute significantly to radar performance by increasing the range of a system for the same amount of radiated power. A functional block diagram of a typical radar RF assembly is shown in Figure 6. The antenna temperature T_A , duplexer loss L_D , and the receiver subsystem noise temperature T_R contributes to the radar system noise temperature T_S as expressed in Equation 1.

$$T_S = T_A + 290 (L_D - 1) + L_D T_R. \quad (1)$$

The current radar technology has been assessed at five specific frequencies. Representative duplexer loss budgets were established, and the



TABLE 3
POTENTIAL APPLICATIONS MATRIX

SYSTEM CATEGORY	FRONT END DETECTION/ VIDEO DETECTOR	FRONT END DETECTION/ HETERODYNE MIXER	LOW NOISE PREAMPLIFIER/ PARAMETRIC AMPLIFIER	LOCAL OSCILLATOR
SEARCH RADAR		X	X	
FIRE CONTROL RADAR		X	X	
ARM SEEKER	0	X	X	X
COMMUNICATION RECEIVER		0		
EW SURVEILLANCE RECEIVER	0		X	
RADIOMETER RECEIVER		0		

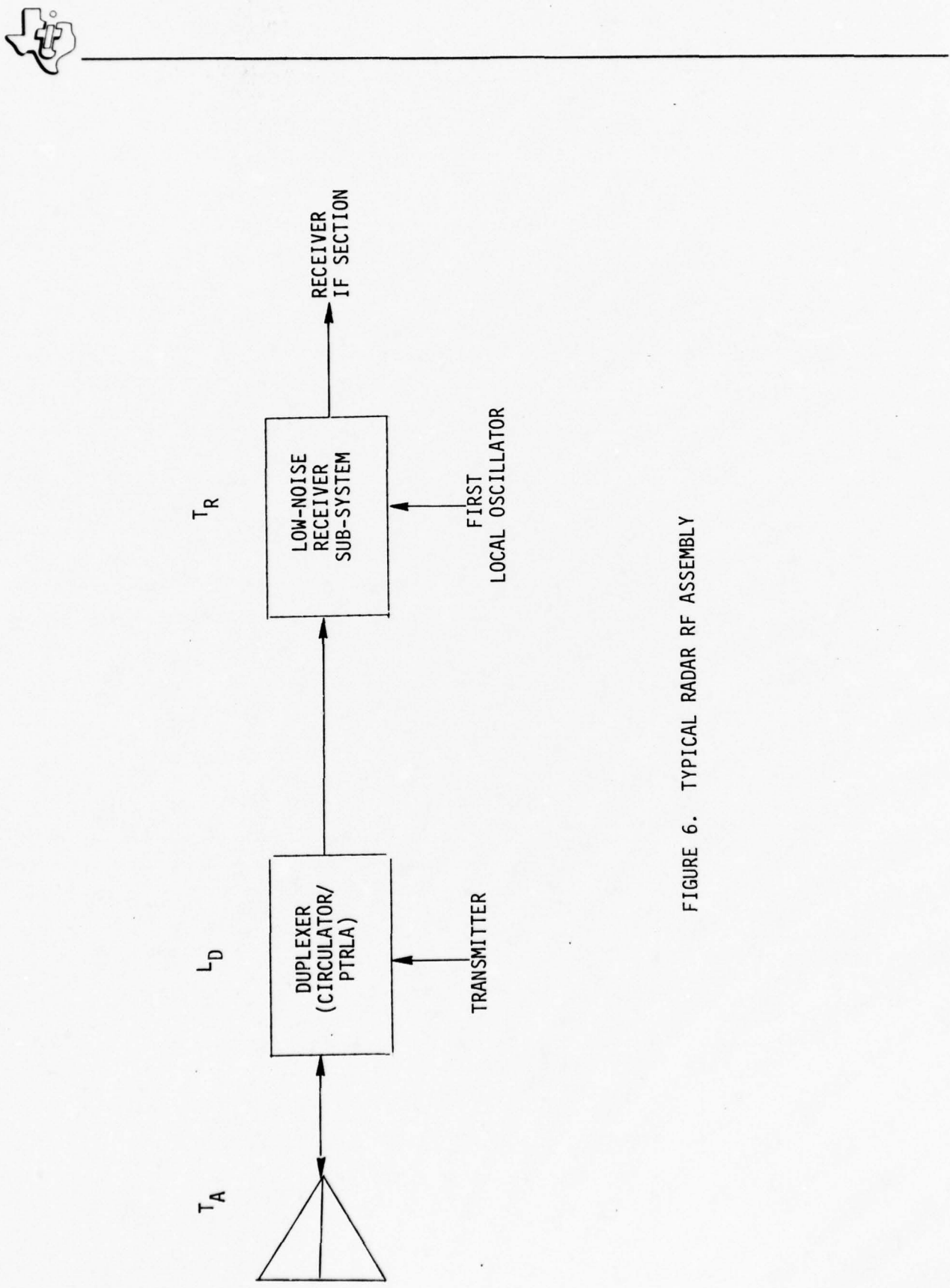


FIGURE 6. TYPICAL RADAR RF ASSEMBLY



non-cryogenic parametric amplifier implementation of the low noise receiver function was selected as a current, medium-complexity system approach. Effective antenna temperatures were established for the five systems assuming a surface based system with a beam pointed several degrees above the horizontal. The results of this study are summarized in Table 4. The low noise receiver temperature includes the parametric amplifier, mixer and IF amplifier noise temperatures.

TABLE 4
CURRENT RADAR RECEIVER NOISE PARAMETERS

FREQUENCY (GHz)	ANTENNA TEMPERATURE (K)	DUPLEXER LOSS (dB)	LOW NOISE RECEIVER TEMPERATURE (K)
3	40	1.5	40
10	40	2.0	80
15	60	2.2	110
37	130	2.6	360
94	200	3.0	770

A system operating temperature was calculated for each system of Table 4. Another system temperature was calculated assuming a perfect receiver but with the same antenna temperature and duplexer losses. The increased range resulting from substitution of the perfect receiver is the maximum improvement that could be gained from the use of Josephson effect devices in a low noise receiver. These results are given in Table 5.

TABLE 5
RADAR RANGE IMPROVEMENT WITH PERFECT RECEIVER

FREQUENCY (GHz)	SYSTEM TEMPERATURE (K)	SYSTEM TEMPERATURE WITH PERFECT RECEIVER (K)	RADAR RANGE IMPROVEMENT (PERCENT)
3	217	160	8
10	336	210	12
15	433	251	15
37	1023	368	29
94	2030	490	43



A maximum improvement of 43 percent could be realized at 94 GHz by replacing the non-cryogenic parametric amplifier with a perfect Josephson device. In practice, quantum noise ($\sim 5-10K$) and atmospheric attenuation would reduce this improvement factor. A system disadvantage associated with the use of Josephson devices is the loss of receiver dynamic range.

In addition, radar receiver applications expose the receiver component (mixer or parametric amplifier) to a relatively large leakage energy from the transmitter pulse. The component must not suffer permanent degradation and must recover to its optimum sensitivity condition within a few microseconds of the termination of the transmitter pulse. Due to the extremely small signal characteristics of Josephson effect devices, it is doubtful that successful operation could be achieved in a radar type environment. In conclusion, the potential improvement factor/increased complexity trade-off does not favor application of Josephson devices to radar receivers.

3. Communication Receiver

The application of superconducting devices in the form of heterodyne mixers to a military communication satellite to ground or sea based terminal is considered in this section. A 500 MHz frequency band centered at 7.5 GHz must be covered by a receiving system of this type. The small signal levels and lower dynamic range requirements are more compatible with Josephson mixer limitations than are radar type applications.

The RF assembly of a communication system is identical to that shown in Figure 6 with the exception that the duplexer becomes a diplexer. The up link transmit frequency covers the frequency spectrum from 7.925 GHz to 8.425 GHz.

The ratio of antenna gain to the receiver system noise temperature (G/T_S) is the major term determining system performance that can be influenced by superconducting mixer technology. In the G/T_S ratio, the antenna gain, G , and the system noise temperature, T_S , are the principal factors. There are



three contributors to the system noise temperature: the antenna temperature, T_a ; the insertion loss, L_D , of the diplexer and feeder system; and the noise temperature, T_R , of a high-gain ultra-low noise amplifier. The relationship between these parameters is expressed by Equation 1.

Principal contributors to noise temperature of a parabolic antenna include cross-polarization loss, forward spillover loss, and aperture blockage and scattering loss. The antenna looks into a sky having various temperature values ranging from 3.5 K at the zenith to 240 K at the horizon. The antenna will sum various noise contributions depending on elevation angle, beamwidth, side lobes, and back lobes and provide antenna noise temperature, T_a . On the average, the antenna noise temperature can be expected to be in the 30-60 K range. The diplexer and feeder loss will never be less than 0.2 dB for earth terminals in this frequency range. Conventional low-noise noncryogenic parametric amplifiers capable of providing the full 500 MHz instantaneous bandwidth are currently used on existing earth terminals. Noise temperatures of 80 K are achieved. Considering the worst case antenna temperature, the system noise temperature would be 157.5K. Cryogenic parametric amplifiers can provide noise temperatures of 35 K in the frequency range of interest. The system noise temperature will be 110.3 K under this condition.

To evaluate the performance a superconducting mixer could provide in this situation, two examples will be considered. The first example will use the mixer performance achieved by M.McColl et.al.²⁵ at 9 GHz, i.e., a mixer noise temperature (T_m) of 6 K and a conversion loss (L_c) of 7 dB. The second example assumes the performance observed at 36 GHz by Y. Taur et.al.²⁶ can be achieved at 7.5 GHz, i.e., a mixer noise temperature of 54 K and a conversion gain of 2.5 dB. For the case of a heterodyne receiver system, the system noise temperature can be calculated from Equation 2.

$$T_s = T_a + (L_D - 1)290 + L_D (T_m + L_c T_{if}), \quad (2)$$

where T_{if} is the noise temperature of the intermediate frequency (IF) amplifier that follows the mixer. The importance of a low IF amplifier noise temperature



is apparent from Equation 2. For the two examples under consideration, a cryogenic parametric amplifier with a 500 MHz bandwidth at 3.95 GHz and a 20 K noise temperature will perform the IF amplifier function. The results calculated for the two examples using Equation 2 are shown in Table 6. The two conventional parametric amplifier receiver systems considered above are included for comparison.

Table 6

Satellite Communication Receiver Comparison

System	T_a	$(L_D - 1)290$	$L_D(T_m + L_c T_{if})$	T_s
Example 1	60	13.7	1.047(6.0+5.01X20.0)	185.0
Example 2	60	13.7	1.047(54.0+0.56X20.0)	141.5
Noncryogenic Paramp (7.5GHz)	60	13.7	1.047(80.0)	157.5
Cryogenic Paramp(7.5 GHz)	60	13.7	1.047(35.0)	110.3

An examination of Table 6 reveals that the conventional cryogenic parametric amplifier will provide the best system performance. Example 2, using a Josephson point contact mixer, provides better performance than the noncryogenic parametric amplifier, and if the mixer performance could be improved to a mixer noise temperature of 33 K with an associated gain of 10 dB, its performance would equal that of the cryogenic parametric amplifier.

A Josephson mixer driven by a local oscillator at the optimum performance level of approximately -60 dBm would demonstrate saturation effects (compression) at an IF output level of -70dBm. With a mixer conversion gain of 10 dB the saturation effect would be observed at an input signal level of -80 dBm. The thermal noise power associated with a 500 MHz bandwidth and a temperature of 73.7 K will be -93 dBm. The dynamic range of this hypothetical system would be 13 dB; a value that is too low for practical applications.

In conclusion, it is felt that superconducting mixers offer no performance improvement over conventional approaches for satellite communication receiver applications.



4. Electronic Warfare Applications

Several naval electronics systems in the 1 GHz to 100 GHz frequency range require the use of broadband video detectors to achieve the performance level dictated by mission requirements. These systems fall within the general category of Electronic Warfare (EW) systems. Certain implementations of two types of EW systems, the Radar Warning Receiver (RWR) and the Anti-Radiation Missile (ARM) use broadband video detectors to sense the presence of pulsed electromagnetic radiation. A study was performed to define the detectability that is presently achieved with conventional detectors and to assess the potential improvement a Josephson or super-Schottky video detector might provide.

The customary measure of video detectability is tangential signal sensitivity (TSS), defined as the ratio of the peak power of the detected pulse to the r.m.s. noise power at the output of the detector video amplifier. Another measure of video detector sensitivity is noise equivalent power or NEP, defined as the input signal power (to the detector) necessary to achieve a final signal-to-noise ratio of unity for a detecting interval or integration time of one second. For a square-law detector, the noise equivalent power is directly proportional to the square root of the post-detection bandwidth, i.e., the NEP decreases as the square root of the final integration time. The equation that relates tangential sensitivity to NEP is:

$$\log_{10}(\text{TSS}) = \log_{10}(\text{NEP}) + 0.5 \log_{10}(B) + 0.4, \quad (3)$$

where B is the postdetection bandwidth in terms of an ideal low pass filter and TSS is expressed for the same postdetection bandwidth.

An NEP of 5.4×10^{-16} watts/ $\sqrt{\text{Hz}}$ has been reported for a super-Schottky video detector operating at 10 GHz²⁵. The theoretical response of Josephson video detectors at 10 GHz is approximately 1×10^{-18} watts/ $\sqrt{\text{Hz}}^2$. The tangential sensitivity for a 5 MHz postdetection bandwidth is computed from equation 3 as

$$\text{TSS} = -85.2 \text{ dBm for an NEP of } 5.4 \times 10^{-16} \text{ watts}/\sqrt{\text{Hz}},$$



and

$$TSS = -112.5 \text{ dBm} \text{ for an NEP of } 1 \times 10^{-18} \text{ watts/}\sqrt{\text{Hz}},$$

where dBm is the power in dB relative to one milliwatt.

The present EW systems use silicon or GaAs Schottky barrier video detectors. These detectors are characterized by a figure of merit that can be related to TSS for a given video amplifier noise figure and bandwidth (postdetection bandwidth). Average diodes at 10 GHz have a figure of merit of $50 \text{ watt}^{-1/2}$, good diodes $100 \text{ watt}^{-1/2}$, and state-of-the-art diodes $200 \text{ watt}^{-1/2}$. For a video amplifier noise figure of 4 dB and a bandwidth of 5 MHz, the TSS becomes -48.7 dBm , -51.5 dBm , and -54.5 dBm respectively. It is apparent that an improvement in tangential signal sensitivity of 25 dB could be realized by using a super-Schottky detector in place of a state-of-the-art room temperature Schottky barrier diode. Since detectability is inversely proportional to the square of the range, a 30.7 dB improvement increases the detection range by a factor of 34.3.

However, the present EW systems have improved detectability by using RF preamplification prior to the video detector. A simplified block diagram of the preamplifier/video detector scheme is shown in Figure 7.

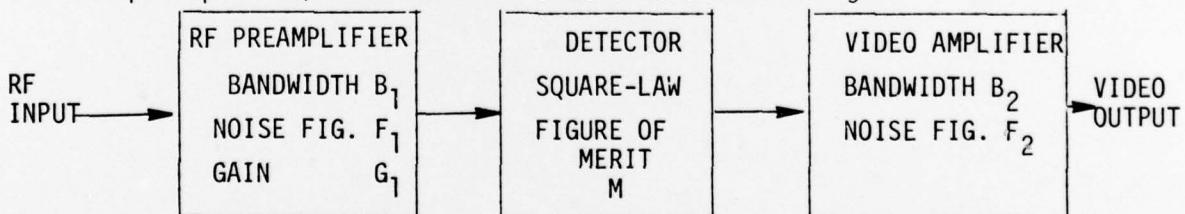


Figure 7. Block Diagram of Amplifier/Detector System

The equations that express the overall tangential signal sensitivity in terms of the preamplifier, detector, and video amplifier parameters are derived by W. J. Lucas.²⁸ The TSS was calculated for several typical preamplifier gain/noise figure combinations. For all cases considered the RF bandwidth, video bandwidth, and video noise figure were held constant at 4 GHz, 5 MHz, and 4 dB respectively. The results of the calculations are shown in Table 7.



TABLE 7

TANGENTIAL SIGNAL SENSITIVITY MATRIX
(dBm)

RF AMPLIFIER CHARACTERISTICS G_1 (dB) F_1 (dB)	VIDEO DETECTOR FIGURE OF MERIT (WATTS) $-1/2$			SUPERCONDUCTING DETECTOR NEP WATTS/Hz $^{1/2}$	
	50	100	200	2×10^{-15}	5×10^{-16}
NO RF AMPLIFIER	-48.7	-51.5	-54.5	-79.5	-85.2
TYPICAL TWT AMPLIFIER (25 dB) (13 dB)	-72.8	-74.6	-75.4		-112.5
TYPICAL FET AMPLIFIER (25 dB) (8 dB)	-73.4	-76.2	-78.5		
ADVANCED FET AMPLIFIER (30 dB) (5 dB)	-78.3	-80.8	-82.6		



The super-Schottky performance of -85.2 dBm exceeds the advanced FET amplifier/detector combination by 2.6 dB. A detection range improvement of 35 percent is associated with the 2.6 dB differential.

The calculations shown in Table 7 assume that system performance is not affected by the antenna noise temperature or losses between the antenna terminals and the input to the RF preamplifier. Also, implied is the fact that the superconducting video detector NEP includes the video amplifier noise figure contribution.

It can be concluded that the potential exists for superconducting video detectors to improve the detection range of EW systems. Since broadband frequency coverage is required for these applications, it is important that the device RF impedance exceed 5 - 10 ohms. The ARM application requires accurate amplitude tracking between matched detector pairs and imposes significant manufacturing producibility constraints. In addition, during the terminal phase of the ARM flight and under certain handling conditions, the RF circuits are subjected to high incident radiation. Protection for the superconducting detector in this environment will require a unique approach.

Two EW systems were selected as possible candidates for increased effectiveness through the application of super-Schottky video detectors. The pertinent system parameters were established and compared with the present and projected performance characteristics of the superconducting detector. Improvement in system performance was projected where applicable. Due to the classified nature of the system parameters, the details of this study are included under separate cover as Appendix A.

5. 94 GHz Radiometer

Study efforts conducted during Phase I have consistently indicated that systems operating in the 60 GHz and greater frequency range offer a much higher probability that the application of superconducting device technology will significantly improve their performance. To some extent, this is due



to the immature state of component and system technology at these frequencies. It was decided that a hypothetical 94 GHz radiometer should be considered as a potential system.

The receiver figure of merit, $(B_{hf})^{1/2}/T_{sn}$, where B_{hf} is the RF bandwidth and T_{sn} is the system noise temperature, is the system parameter that can be improved by application of superconducting device technology. A conventional radiometer using a mixer followed by an IF amplifier with a 1.5 dB noise figure and a 2 GHz bandwidth would have an equivalent (double sideband) noise bandwidth of 5.2 GHz. A mixer conversion loss of 6 dB would result in a system noise temperature of 1638 K. The receiver figure of merit would be $44 (K^2 \cdot sec)^{-1/2}$. For a one second integration time, the figure of merit corresponds to a minimum detectable temperature change of 0.023 K.

Josephson point contact video detectors have demonstrated NEP's in the 3 to 5×10^{-15} W/\sqrt{Hz} range at frequencies near 94 GHz.^{2,29} If it is assumed that an NEP of $10^{-15} W$ can be achieved over a 10 GHz frequency range at 94 GHz, a radiometer system could be configured with a minimum detectable temperature change of 0.0073 K. The receiver figure of merit would be $153 (K^2 \cdot sec)^{-1/2}$.

The radiometer detection range is proportional to the receiver figure of merit raised to the 2/3 power. The improvement factor in detection range that would be achieved using Josephson video detectors is 2.3. As with all systems considered in this study, the saturation characteristics of the superconducting detector must be considered. A radiometer with a 10 GHz bandwidth and looking at the earth (290 K) will have an incident power level on the detector of -74 dBm.

It is apparent that incoherent video detectors using Josephson point contacts can offer detection range improvement in radiometer applications at 94 GHz. A video detection system would be much less complex electrically than a heterodyne system and should be competitive from a cost standpoint including the cryogenic requirements. The video detector approach could include an array of detectors arranged along a focal plane in a common cryogenic system. Multiple beam coverage could then provide a larger field of view for the same integration time with little additional system complexity.



6. Processing for Radar Imagers

Present radar systems operating in the 9 to 18 GHz frequency range are capable of instantaneous frequency bandwidths of 500 MHz or greater. However, at the present time processing speeds are not compatible with handling information rates of this magnitude. A coherent radar operating with a 500 MHz bandwidth could provide doppler information on range cells of one foot resolution. A 9 bit analog-to-digital (A/D) converter would be required to provide a dynamic processing range of 54 dB. To handle the full 500 MHz bandwidth with 9 bit resolution, two A/D converters working on in-phase and quadrature - phase components would be required to clock at a 4.5 GHz rate. Processing the digitized information will require a high speed digital computer with an extensive memory. Superconducting cryotrons have been shown to operate fast enough to implement logic functions at these clock rates and considerable attention is being given to superconducting memories employing Josephson devices.

F. Above 100 GHz

Much of the potentially improved detection capabilities shown for a 94 GHz system applies equally well to systems operating above 100 GHz. However, atmospheric attenuation is much greater and probably excludes any earthbound military application above 300 GHz. No present Navy system operating in this frequency region are known.



SECTION III

CONCLUSIONS AND RECOMMENDATIONS

Several candidate Naval surveillance and communication systems have been identified where the use of Josephson effect devices might contribute significantly to improved performance. Two potential applications (MAD and ELF communications) have already received considerable attention and should have continued support. Two processing applications deserve further consideration but should probably be included in a comprehensive digital processing development program for cryogenic devices.

At high frequencies (>1 GHz) several potential applications have been identified where the use of Josephson effect devices might yield substantially improved performance. In calculating possible performance no consideration was given to the practicality of using cryogenic devices, and for some applications a breakthrough in refrigeration technology or superconductor critical temperatures may be required.

The data available on superconducting devices in the open literature emphasized the low noise operating characteristics of the devices. Data concerned with high level power handling capability, sensitivity to shock and vibration, and reliability were not available. All these factors are important when considering operation in a military system environment. It is recommended that the Phase II effort be structured to address in a preliminary manner these additional areas. Also, the performance data were specified on the devices essentially separated from the circuit test environment. Obviously, the application to a specific system must include the associated circuitry and its attendant degradation of device performance. A more detailed study in this area is necessary.

We believe a 94 GHz imager deserves serious consideration for support in succeeding phases of this program and therefore make the following recommendations.



A. 94 GHz Real Time Image System

The 94 GHz video detector array appears to have high potential impact and a reasonable probability of success. Whether such a receiver is used passively or with an illuminator will depend upon the particular application. Relatively high power sources are being developed which could be used as illuminators. The significance of 94 GHz (wavelength 3.2 mm) is that this is the highest frequency atmospheric window with a sealevel attenuation (≈ 0.4 dB/km) of less than 1 dB/km. It therefore offers the highest spatial resolution for imaging through haze, smoke or fog where infrared or optical instruments no longer function. No in-service systems presently operate at this frequency but when developed, this system could significantly enhance the capability of or replace existing fire control and surveillance systems.

Recommendations:

1. Develop preliminary 94 GHz imaging system design to include scan technique, array size, resolution, and display.
2. Perform detailed study of system requirements, specifying NEP, bandwidth and other electrical parameters.

The following general recommendations are made for other programs that show significant potential application.

B. Magnetic Anomaly Detection (MAD)

The high stable balance and alignment required for MAD gradiometers can probably only be obtained by fabricating SQUIDs and sense loops with thin film photolithographic techniques. This requires the development of planar Josephson junctions and planar SQUIDs. This work has started with development of thin film superconducting gradiometer loops and should be continued to include thin film SQUIDs. Also important to determining feasibility is an analysis of the processing required to convert magnetic gradient signals in the presence of noise into useful information.

Recommendations:

1. Develop techniques for fabricating superconducting thin film gradiometer sensors using precision photolithography.



2. Develop algorithms to extract tactical parameters from gradiometer signals.

3. Measure gradient noise.

C. ELF Communications

Even though transmitter antenna location and construction is presently uncertain, the potential advantages of Josephson device receivers are sufficiently great to justify continued development of an ELF receiver. Preliminary specifications of required electrical parameters have already been made.

Recommendations:

1. Conduct theoretical and experimental comparison of Josephson effect devices to determine the best device for ELF receivers.

2. Investigate various sensor configurations and their influence on required dynamic range and construction precision.

D. Fast Digital Processing

The high speed and low power consumption of Josephson device digital processing elements has stimulated considerable development effort - particularly for very large computers. Certainly this work should be continued. Two applications have been discussed where the fast processing alone would permit performance of a task not possible with conventional components. Both real time correlation processing of a data stream and processing of a high range resolution radar require very fast A/D converters and adders.

Recommendations:

1. Continue present digital processing development.

2. Design, fabricate and test fast Josephson A/D converters.

E. Electronic Warfare Systems

A potential improvement in anti-radiation missile (ARM) seekers employing Josephson technology has been shown; however, the increase in range



over what could probably be achieved with improved conventional detectors was not considered significant enough to justify pursuing the problems of dynamic range and cryogenic logistics that would be introduced. Details supporting this conclusion are contained in the classified appendix.



REFERENCES

1. Tinkham, M., *Introduction to Superconductivity*, McGraw-Hill, New York (1975).
2. Kanter, H., and Vernon, F.L., *J. Appl. Phys.* 43, 3174 (1972).
3. Kanter, H., *J. Appl. Phys.* 46, 2261 (1975)
4. Parrish, P. T., and R.Y. Chiao, *Appl. Phys. Letters* 25, 627 (1974).
5. Silver, A. H., *IEEE Trans. Magnetics* MAG-11, 794 (1975).
6. Matisoo, J., *Proc. IEEE* 55, 172 (1967)
7. Zappe, H. H. and K. R. Grebe, *J. Appl. Phys.* 44, 865 (1973)
8. Jutzi, W., Th. O. Mohr, M. Gasser, and H. P. Geschwind, *Electronics Letters* 8, 589 (1972)
9. Zappe, H. H., *IEEE J. Solid-State Circuits* SC-10, 12 (1975)
10. Broom, R. F., W.Jutzi, and Th. O. Mohr, *IEEE Trans. Magnetics* MAG-11, 755 (1975)
11. Henkels, W.H., *IEEE Trans. Magnetics* MAG-10, 860 (1974); D. J. Herrell, *IEEE J. Solid-State Circuits* SC-9, 277 (1974)
12. Herrell, D.J., *IEEE Trans. Magnetics* MAG-10, 864 (1974)
13. Herrell, D.J., to be published.



REFERENCES

(Continued)

14. Wynn, W.M., "Dipole Tracking with a Gradiometer", Informal Report NSRDL/PC3493, Jan. 1972 (UNCLASSIFIED) and W. M. Wynn, C.P. Frahm, P. J. Carroll, R. H. Clark, J. Wellhoner, and M. J. Wynn "Advanced Superconducting Gradiometer/Magnetometer Arrays and a Novel Signal Processing Technique." IEEE Trans, on Magnetics, MAG-11, 701, (1975).
15. Klein, F., Journal fur Mathematic, 129, 15 (1905).
16. Klein, F., Mathematische Annalen, 61, 50 (1905).
17. Michael, Mike, "Compendium on MAD Signal Processor" Texas Instruments Incorporated, Memorandum TM74-025 (U), June 1974
18. Overton, Jr., W.C., "Signal Physics of Magnetic Anomaly Detection (MAD) by Superconducting Gradiometer (U)." Los Alamos UC, Informal Report LA-5522-MS (CONFIDENTIAL)
19. Clement, J. R., E. M. Compy, and M. Nisenoff, "Some Practical Consequences of Platform Instability for a Superconducting Gradiometer MAD System." NRL Memorandum RPT 2648 (October 1973)
20. Keiser, B. E., IEEE Transactions on Communications, Vol. Comm. 22, No. 4, (1974)., 364.
21. See for example Harrison E. Rowe. Ibid., 371.
22. Wolf, S. A., J. R. Davis and M. Nisenoff. Ibid., 549. Davis, J. R., and M. Nisenoff, "SQUID Magnetometers for Submarine Communications at Extremely Low Frequencies", IC SQUID, Berlin, October, 1976.



REFERENCES

(Continued)

23. Welker, N. K., F. D. Bedard, NRL Report 7822, Proceedings of 1973 Workshop on Naval Applications of Superconductivity.
24. E. A. Wolff, Antenna Analysis, John Wiley & Sons, N.Y. (1966), pp 262-266.
25. M. McColl, M.F. Millea, A.H. Silver, M.F. Bottjer, R.J. Pedessen, F.L. Vernon, IEEE Trans. Magnetics MAG-13, 221 (1977).
26. Y. Taur, J.H. Claassen, P.L. Richards, IEEE Trans. Microwave Theory and Techniques MTT-22, 1005 (1974).
27. J. Clarke, Private Communication.
28. W.J. Lucas, Proc. IEEE 113, 1321 (1966).
29. H. Tolner, C.D. Andriesse, H.H.A. Schaeffer, Infrared Phys. (G.B.) 16, 213 (1976).

UNCLASSIFIED

SECURITY CLASSIFICATION OF THIS PAGE (When Data Entered)

REPORT DOCUMENTATION PAGE		READ INSTRUCTIONS BEFORE COMPLETING FORM
1. REPORT NUMBER	2. GOVT ACCESSION NO.	3. RECIPIENT'S CATALOG NUMBER
4. TITLE (and Subtitle) Josephson Junction Technology Program, Phase I.		5. TYPE OF REPORT & PERIOD COVERED Final Report 10/4/76 - 4/21/77
7. AUTHOR(s) Forrest D. Colegrove, Jerry D. Holmes Spencer A. Buckner, ✓ David N. McQuiddy		6. PERFORMING ORG. REPORT NUMBER N/A
8. PERFORMING ORGANIZATION NAME AND ADDRESS Texas Instruments Incorporated Equipment Group, P.O. Box 6015 Dallas, Texas 75222		9. CONTRACT OR GRANT NUMBER(s) 15 N00173-76-C-0388
11. CONTROLLING OFFICE NAME AND ADDRESS Naval Research Laboratory Cryogenics & Superconductivity Branch Code 6435 4555 Overlook Ave., S.W., Washington, DC 20375		10. PROGRAM ELEMENT, PROJECT, TASK AREA & WORK UNIT NUMBERS 11 21 Apr 77
14. MONITORING AGENCY NAME & ADDRESS (if different from Controlling Office) Chief DCASO Texas Instruments Inc. P.O. Box 6015, MS 256 Dallas, Texas 75222		12. REPORT DATE 4/21/77
		13. NUMBER OF PAGES 56
		15. SECURITY CLASS. (of this report) Unclassified
		15a. DECLASSIFICATION/DOWNGRADING SCHEDULE NA
16. DISTRIBUTION STATEMENT (of this Report) Approved for Public Release Distribution unlimited		
17. DISTRIBUTION STATEMENT (of the abstract entered in Block 20, if different from Report) Same		
18. SUPPLEMENTARY NOTES		
19. KEY WORDS (Continue on reverse side if necessary and identify by block number) Josephson Devices Superconductivity Surveillance Systems Communication systems		
20. ABSTRACT (Continue on reverse side if necessary and identify by block number) A search has been made of Naval surveillance and communications systems in the frequency range DC to above 100 GHz for the purpose of identifying systems in which the application of Josephson effect devices might improve performance. Magnetic anomaly detection, ELF communications, fast digital processing and some radar applications were examined and found to be potential candidates for superconducting devices. Analyses of systems considered and rejected are also included.		

405076

JB